

INFORMATION TECHNOLOGY, COMPUTER SCIENCE, AND MANAGEMENT



Original article

<https://doi.org/10.23947/2687-1653-2022-22-3-261-271>

Describing Pulmonary Nodules Using 3D Clustering

Amera Al-Funjan¹ , Farid Meziane² , Rob Aspin³

¹Babylon University, Iraq

²University of Derby, Derby, UK

³Manchester Metropolitan University, Manchester, UK

✉ amera.alfunjan@uobabylon.edu.iq



Abstract

Introduction. Determining the tumor (nodule) characteristics in terms of the shape, location, and type is an essential step after nodule detection in medical images for selecting the appropriate clinical intervention by radiologists. Computer-aided detection (CAD) systems efficiently succeeded in the nodule detection by 2D processing of computed tomography (CT)-scan lung images; however, the nodule (tumor) description in more detail is still a big challenge that faces these systems.

Materials and Methods. In this paper, the 3D clustering is carried out on volumetric CT-scan images containing the nodule and its structures to describe the nodule progress through the consecutive slices of the lung in CT images.

Results. This paper combines algorithms to cluster and define nodule's features in 3D visualization. Applying some 3D functions to the objects, clustered using the K-means technique of CT lung images, provides a 3D visual exploration of the nodule shape and location. This study mainly focuses on clustering in 3D to discover complex information for a case missed in the radiologist's report. In addition, the 3D-Density-based spatial clustering of applications with noise (DBSCAN) method and another 3D application (plotly) have been applied to evaluate the proposed system in this work. The proposed method has discovered a complicated case in data and automatically provides information about the nodule types (spherical, juxta-pleural, and pleural-tail). The algorithm is validated on the standard data consisting of the lung computed tomography scans with nodules greater and less than 3mm in size.

Discussion and Conclusions. Based on the proposed model, it is possible to cluster lung nodules in volumetric CT scan and determine a set of characteristics such as the shape, location and type.

Keywords: automated 3D Clustering, CT lung images, describing the nodule characteristics.

Acknowledgements. The authors would like to thank the reviewers for their suggestions that improved the article.

For citation. Amera Al-Funjan, Farid Meziane, Rob Aspin. Describing Pulmonary Nodules Using 3D Clustering. Advanced Engineering Research, 2022, vol. 22, no. 3, pp. 261–271. <https://doi.org/10.23947/2687-1653-2022-22-3-261-271>

Introduction. Lung cancer is a leading cause of death worldwide among both men and women, with an impressive rate for nearly 10 million deaths in 2021. Around one-third of deaths from cancer are to smoking and second-hand smoke. Many cancers can be cured if detected early and treated effectively (1).

Computed Tomography (CT) is one of the most commonly medical imaging techniques used in the screening of lungs by generating three-dimensional imaging modalities and shows the lesions that cannot be visualized by conventional chest X-ray. CT technology is used widely by clinicians to detect, analyze, and diagnose numerous asymptomatic disease lung diseases such as pulmonary nodules and lung cancers, that cannot be detected by other

medical imaging technologies. Where, early detection of these diseases is an important of health promotion and chronic disease prevention. However, it is noted that a big challenge associated to radiologists is the analysis of huge amount of data generated by CT technology. Therefore, computer-aided diagnostic (CAD) is needed to provide a computerized diagnosis to assist clinicians for detection and interpretation of CT lung scans (2, 3). Segmentation and clustering are tasks that manipulate the medical image to extract significant information and reduce the search area of the region of interest in image components. Where, using clustering on volumetric scan of CT can provide more details about nodule shapes, characteristics, and their types which are suspected be missed by radiologists during the diagnosis. Additionally, it provides a precise description of lung's tissues with low-intensity (4, 5). The outcomes of 3D clustering can improve the precision in diagnosis of lung by identifying the nodule structures in the different levels, and the number of nodules (6, 7). This study aims to improve the accuracy of three-dimensional clustering of lung's nodules by using volumetric CT scans of lung. Where, the three-dimensional clustering efficiently can be used to observe the current nodule's progress which serves significantly the early diagnosis of lung. Furthermore, the precise details that can be extracted from the three-dimensional clustering offers a high potential to detect nodules and lesions with less than 3 mm.

Many studies focused on the possibility of developing a computer-aided system for diagnosing, detecting, and segmenting lung lesions in CT scans of lung (8). However, without using volumetric CT scans of lungs, the accurate identification and characterization of small pulmonary nodules have not been defined in the studies. Where, implementing quantitative analysis of CT scans of lungs face an obstacle due to inter-scan image intensity variations and irregular shapes of lung lesions. A major difficulty is encountered during clustering of lung's lesions because of the complex characteristics of lung's lesions and overlapping in intensity distributions in such cases. Additionally, some parts of lung's lesions may not be distinguished correctly because of the image resolution and the complexity of diagnosing lung's lesions in a visual examination. Therefore, a multi-dimensional CT scan is required to determine type and volume of lesions.

Javaid, Javid (9) proposed an automated method for segmenting and recognizing the pulmonary nodules into juxta-vascular or juxta-pleural. Where, thresholding and k-means were combined to segment lung and detect the pulmonary nodules respectively. Then, the pulmonary nodules were classified into sex groups according to percentage of connectivity with lung walls and thickness. Fetita, Preteux (10) developed a method for discriminating lung's nodules from other dense structures by using volumetric space of the thorax. Where, the achieved false positive rate was 8.5 per exam. Fetita, Preteux (10) applied a three-dimensional active contour method to segment 96 lung's nodules, then the texture features were extracted and classified into classes by a linear discriminant analysis (LDA). Ozekes and Osman (11) suggested a CAD system based on volumetric CT scans of lung to detect lung's nodules which have diameters (3.5–7.3) mm. In this study, four classifiers were used to evaluate the suggested system.

Furthermore, El-Baz, Elnakib (12) exploited the efficacy of genetic algorithm (GA) to isolate nodules, arteries, veins, bronchi and bronchioles from the surrounding anatomical structures based on volumetric and two-dimensional CT lung scans. It was proved that the lung nodules were recognized precisely when using volumetric CT scans. In this study, it was noted that the false positive rate was reduced significantly when utilizing volumetric CT scan of lung compared to two-dimensional CT scan. The achieved sensitivity and false positive rates were 82.3 % and 9.2 % respectively.

In this study, we proposed a new system to describe automatically lung's lesions in volumetric CT scans, as well as, determining the nodule numbers, type location, shape, progress of lesion. The main contribution of this study is to discriminate the complicated lung's nodules that have non seen through the clinical routine. A successful system can improve the accuracy of the diagnosis process. The following research objectives focus on how the above aim will be achieved:

- to extract the most distinct characteristics of the lung's nodule to that helps to determine treatment decisions and predict expected outcomes;
- to detect the complicated lesions cases that cannot be identified with certainty by radiologists;
- constructing an efficient CAD system that can determine precisely lung's nodules number and types.

The rest of this paper is organized as follows. In Section 2, material and method will be described and the conclusion will be discussed in Section 3.

Materials and Methods. The core-aim of the present study was to build an automated algorithm of clustering nodules from CT lung scans in an axial plane. The proposed algorithm is divided into three stages as shown in Fig. 1. First, the CT lung scan undergoes an enhancing process and separating of lung from background in the pre-processing stage. Then, the CT lung scan is clustered in 2D and 3D for detecting the vessel and nodules from normal tissue in the post-processing stage, as well as reducing the area region about nodules in 2D clustering while describes the nodule shape in 3D clustering. The results of 3D clustering are evaluated using two ways (3D-DBSCAN method and Plot.ly application). The evaluation stage confirms the outcomes precision of previous stage (post-processing) in detecting the number and shape of nodules that founded in the complex case, which is recorded in radiologist's report.

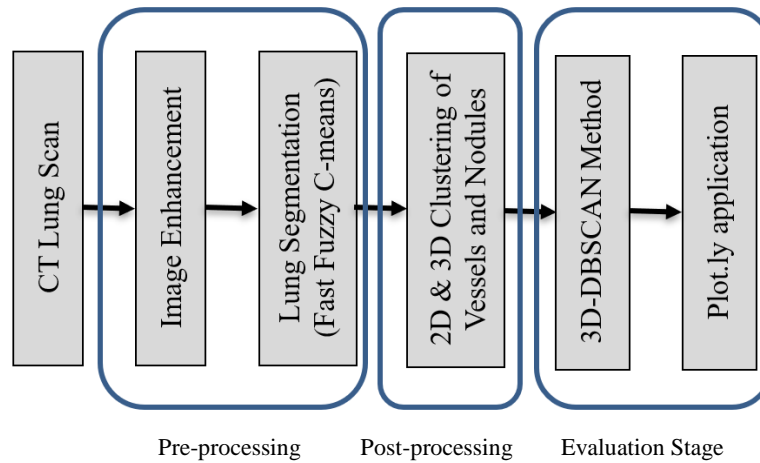


Fig. 1. The Proposed Model of Lung CT scan Clustering

Data Collection This study included 85 lung CT scans with pulmonary nodules, were downloaded from the TCIA (Cancer Imaging Archive) website (13). The provided data was annotated and screened by four radiologists to determine and extract the diagnostic details of lung's nodules such as number, size, location, volume, diameter, type of lung's nodules. In addition to slice number of the pathological lung. Figure 2, shows samples of CT lung scans form the provided dataset in axial viewing.

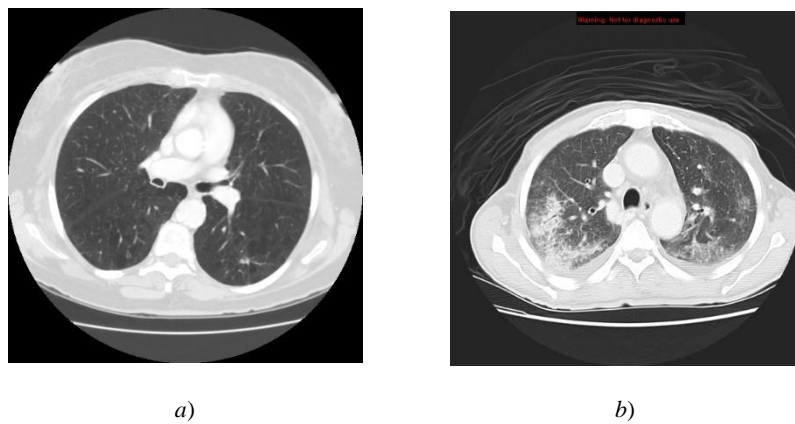


Fig. 2. Lung CT slices in the axial view: *a* — healthy CT lung scan; *b* — pathological CT lung scan

Pre-processing of Lung CT Scan. To reconstruct the CT images, a million of independent detectors are used to collect the x-ray signals. Subsequently, the CT artifacts may be occurred during the reconstruction process. Where, these artifacts cause intensity variations across consecutive re-constructed CT scan slices. Therefore, the lung CT scans are pre-processed by implementing a set of algorithms such as image enhancement by gaussian filter, intensity normalization by histogram normalization method, lung extraction by thresholding (1, 14) as shown in Fig. 3.

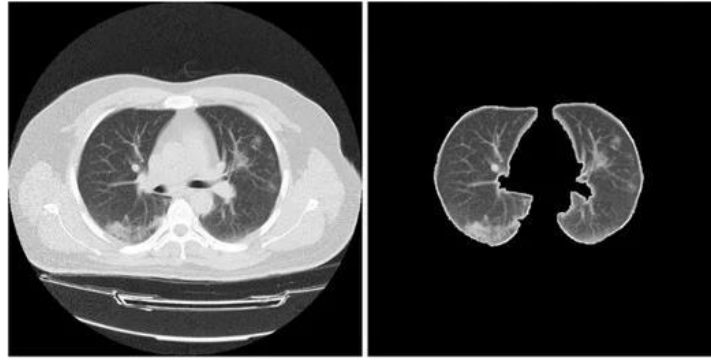


Fig. 3. Lung boundary identification samples: *a* — Original CT image; *b* — Preprocessed CT image

Three-dimensional Clustering. In this step includes implementation of a set of image pre-processing methods to prepare the CT scans of lung more appropriate for implementing the K-mean clustering method. Where, reduction of parenchyma tissue was achieved by isolating the intensity values that represents the vessels and nodules together. Then, vessels and lung's nodules were separated by implementing the K-mean clustering method on each CT image separately. It is an efficient and non-supervised technique that allows the cluster center to shift and fit the ROI (15–17). Subsequently, any hole appearing in the clustered CT scan of lung is removed by implementing a set of morphological operations (1). Then, the clustered CT images of each patient were stacked into single a volumetric CT scan and underwent the 3D graphics functions later.

Finally, a three-dimensional volume reconstruction from cross-sectional CT scans is determined by using isosurface function which was provided by MATLAB and used to measure the geometric computations of clustered data, and improved volumetric visualization of objects. Where, pixel coordination (x, y, z) and intensity values of pixel of each cross-sectional clustered scan was given as input to the function. Moreover, isocaps and isonormal functions were used to enhance produced the three-dimensional representation of the lung's nodules and vessels. Consequently, the three-dimensional clustering stage detects nodules, shape, type, and progress and finds out the unseen lesions in the CT scan of lung. The suggested algorithm was applied to cluster nodules and vessels in volumetric CT scan of lung.

First step was the threshold, where each value of the intensity in the volumetric CT scans by a specific value to extract correctly the lung's nodules from the CT scan of lungs by using Eq. 1.

$$G(x, y) = \begin{cases} 1 & \text{if } P(x, y) > T \\ 0 & \text{Otherwise} \end{cases} \quad (1)$$

Where, $P(x, y)$ indicates the intensity values representing the nodules and vessels which are greater than the threshold value which is set experimentally.

The second step used K-means clustering on each CT lung images individually to eliminate any undesirable holes that occurred in the clustering process. The output of clustering process was labelling pixels of CT images into two main clusters (nodules and vessels). K-means clustering implemented by using the following steps.

1. Initialize k to specify cluster center, $C = c_1, c_2, \dots, c_k$.
2. Determining the distance between CT lung image's pixels and the cluster centers by using Eq. 2:

$$S = \sum_{i=1}^m \sum_{j=1}^n \|x_i - c_j\|^2 \quad (2)$$

where, x_i is an intensity pixel associated with m and n coordinates.

3. Assigning the CT lung's pixel with minimum distance to the nearest cluster's center.
4. Updating the cluster centers according to Equation (3):

$$C_i = \frac{1}{N_{i,j}} \sum_{j=1}^{N_{i,j}} x_{i,j} \quad (3)$$

where, c_i and $N_{i,j}$ indicate the i^{th} cluster center, and all pixels of the i^{th} cluster respectively. While, $x_{i,j}$ signifies all pixels of i^{th} cluster center.

5. Repeating steps 2 to 4 until minimizing the objective function S to the lowest value.

Finally, implemented a three-dimensional function on the labelled clusters of CT images to generate the volumetric data. Where, the volumetric data was plotted according to a set of calculations. The following procedure was used to combine the labeled clusters and produce lung's nodule's shape and type (18). Algorithm 1 shows the pseudo-code for the generating of volumetric lung's nodule steps.

Algorithm 1: Pseudo-code for generating of volumetric lung's nodule.

Input: Clustered image (x,y,z).

Output: Output volumetric figure (i,j,k).

Begin

 Apply *Isosurface* function to present a volume visualization.

 Apply *Isocaps* function to adjust colors of faces of the produced volumetric lung's nodules.

 Apply *Azimuth* and *Elevation* functions to create axes in three-dimensional view.

 Apply *Isonormals* to determine the normal vertices and create a surface shadow through vertices gradient.

Results. The plotted three-dimensional space of lung's nodules enhanced visualization of nodules and vessels and provided more descriptions on the lung's nodules than what extracted by two-dimensional space. Where, the former provides more details regarding shape and locations of lung's nodules. Figure 4, shows an example of pathological lung that has two nodules with a red referral that are appear between slices no. 60 and 64. After implementing the three-dimensional clustering, a thin tissue between lung's nodules that is invisible by two-dimensional clustering, becomes visible to the radiologists. Furthermore, it extends through CT slices no. 61 to 63. Therefore, by depending on the two-dimensional clustering leads to make the inspection process by the radiologist prone to error and may diagnose one lung's nodule as two separated nodules.

Moreover, the proposed system provides more details about the lung's nodule type. Where, each lung's nodule was classified into juxta-vascular and juxta-pleural nodules. Figure 5, reveals how an early lung's nodule was detected and notified and this will help the clinicians to improve patient survival rates. Figure 6 shows how the lung's nodules are connected through their center pixels.

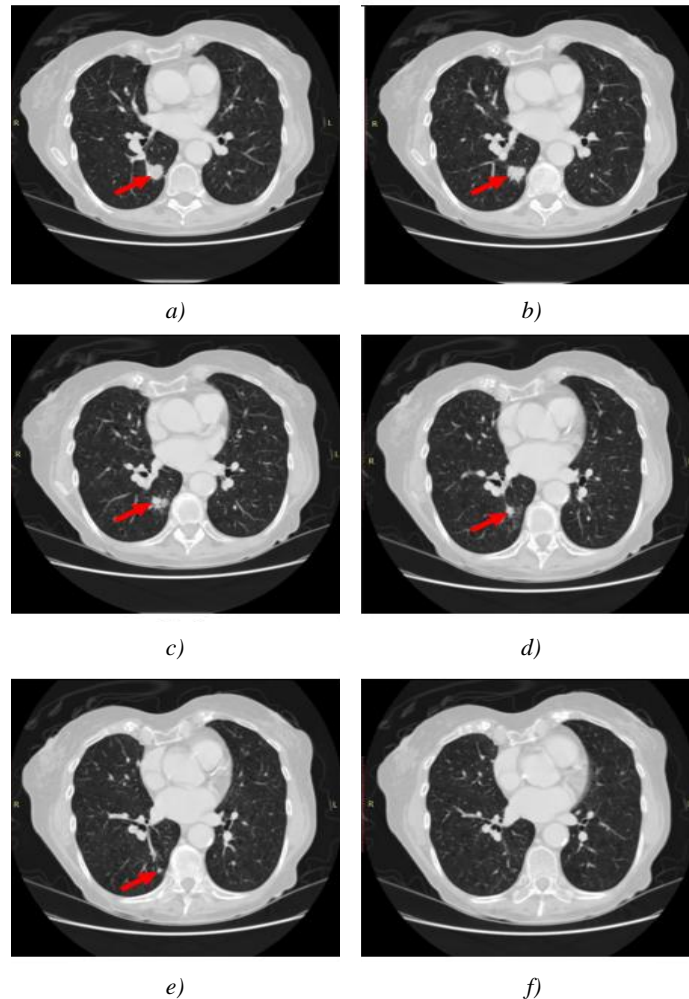


Fig. 4. Original CT Lung scan between Slice 60 and 64 with a Red arrow to indicate Two Attached Nodules: *a* — Candidate Nodule in the 60th slice; *b, c, d* — lung Nodules through slices 61, 62, 63; *e* — Nodule in slice 64; *f* — Normal slice after slice 65

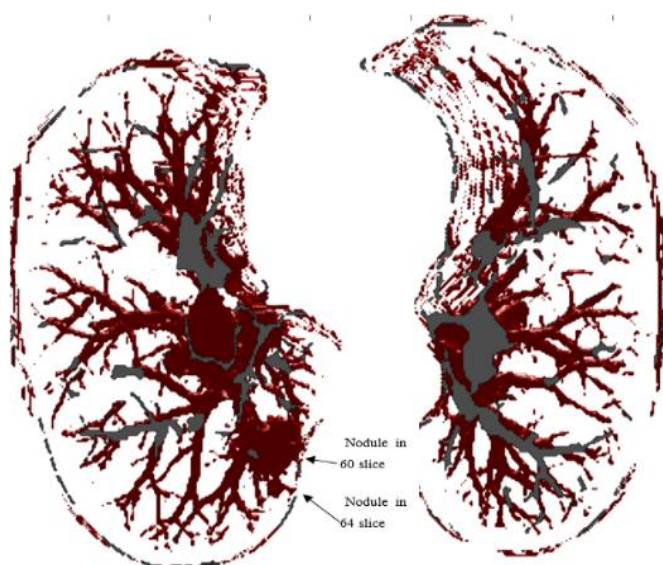


Fig. 5. Three-dimensional Clustering of CT lungs Attached Nodules in 60th and 64th Slices

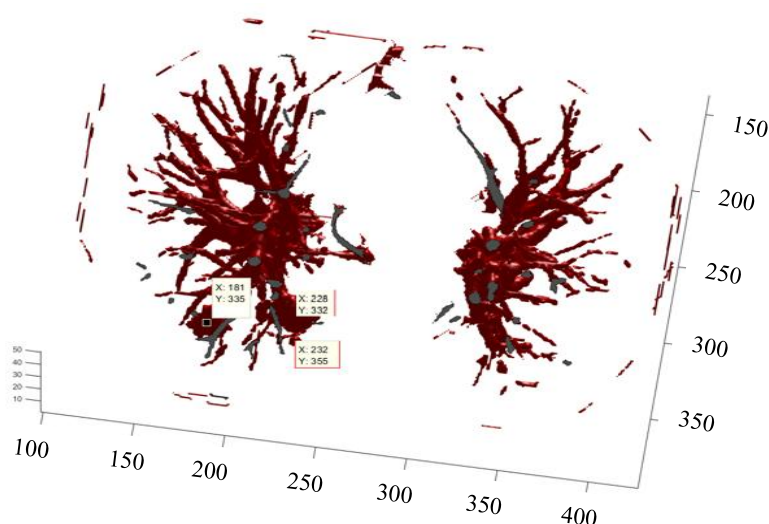


Fig. 6. Three-dimensional Clustering of two lung nodules that are located in different slices

Although the three-dimensional graphic is evaluated visually, it is essential to evaluate quantitatively the quality of the achieved results. The Density-based spatial clustering of applications with noise (DBSCAN) method and 3D plot.ly application were used to evaluate the performance of the proposed three-dimensional clustering method (19, 20).

The DBSCAN method is one of the most popular and standard clustering techniques (21–23). It was used to set of nearby pixels are grouped to gather into a single cluster, and isolate the outlier pixels in a low-density area. The clustering process of this method depends on two key parameters (Epsilon and MinPts) that deal with core point in the volumetric space. Where, Epsilon is the distance that specifies the neighborhoods. Two points are considered to be neighbors if the distance between them is less than or equal to eps. While, MinPts represents minimum number of data points to define a cluster. Then, a point is considered as a core point if there are at least MinPts number of points (including the point itself) in its surrounding area with radius eps.

DBSCAN method was modified to cluster the volumetric CT lung scans to compare its output with the proposed system in this study by comparing the cluster's centers that were achieved by both methods. Where, DBSCAN inspects and connects all objects to the core pixels based on eps and MinPts measures. Synchronously, all the points that do not

represent core points are ignored. Many advantages are achieved by using this method, first, no need to initialize cluster numbers like k-means cluster method. Secondly, random shaped clusters are discovered easily. Finally, if the data is fully understood, it is easily to specify the MinPts and ets parameters.

Fig. 7 shows how the lung's nodules were linked through CT slices. Where, the 3D-DBSCAN method evaluated the connection between attached nodules compare with the clustered lung's nodules of the proposed system in this study. It is noted that the center's pixels were approximately matched as shown in Fig. 8. Fig. 9, shows how the lung's nodules were linked and spread by a thin line between CT slices no. 60th and 64th.

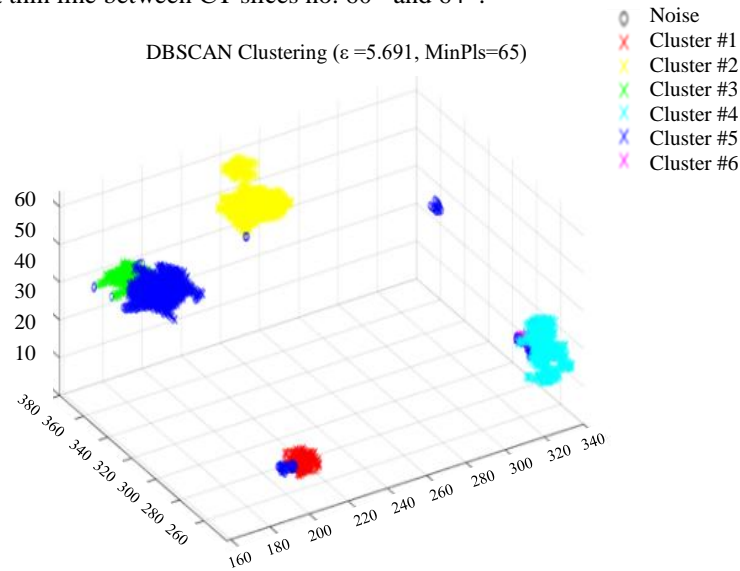


Fig. 7. 3D-DBSCAN clustering Method, yellow cluster refers to Linked Nodules, and other colors refer to the Remaining Nodules of the Same Patient

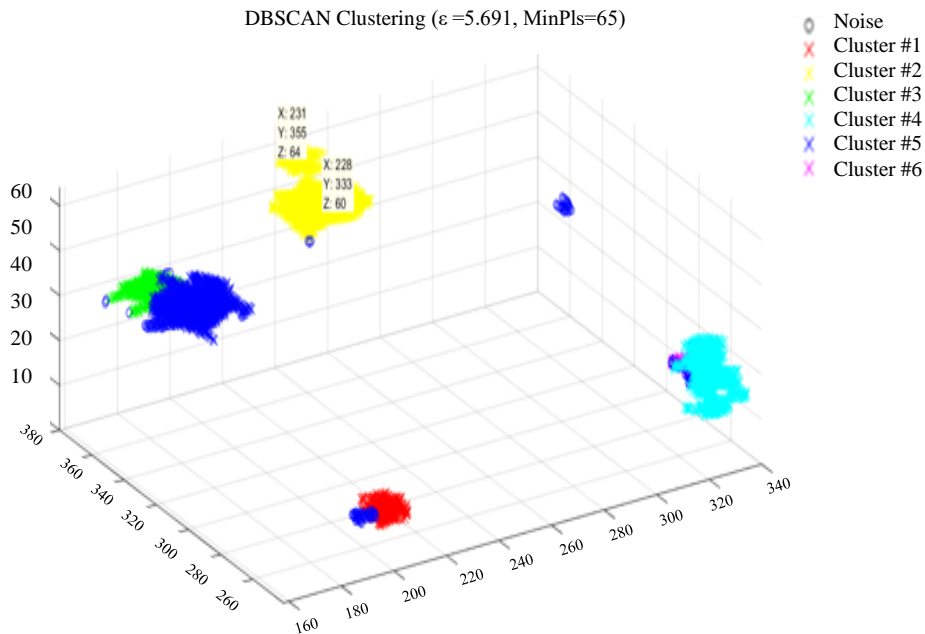


Fig. 8. 3D-DBSCAN clustering Method, yellow cluster refers to the Linked Nodules, Centers Pixels were recognized by Radiologist, and other colors refer to the Remaining Nodules

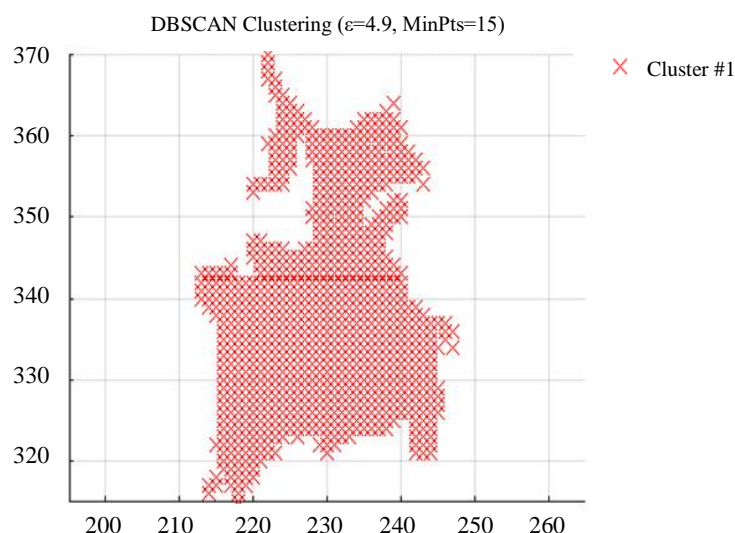


Fig. 9. DBSCAN Method Just Clusters the Linked Nodules and Proves One Nodule

Another 3D application was utilized in this study to evaluate the proposed system. It is named plot.ly application. This application used colored bubbles to locate pixels within the candidate nodule and its structures in different slices, as shown in Fig. 10 and Fig. 11. It was initialized by the coordinates of lung's nodules centers and it extended consecutively through similar structures in neighbor CT slices. Moreover, it was essentially to initialize pixel size and pixel spacing of CT scan, which are determined by Eq. 4 and Eq. 5.

$$\text{Pixel spacing}(x - \text{size}, y - \text{size}) = \left(\frac{(\text{Field of view(FOV)})}{(\text{Matrix Size})} \right)^2 = \left(\frac{360\text{mm}}{512} \right)^2 = 0.703^2 \quad (4)$$

$$\text{voxel size} = \text{pixel spacing}(x - \text{size}) \times \text{pixel spacing}(y - \text{size}) \times \text{thickness} = 0.703 \times 0.703 \times 2.5 = 1.235 \quad (5)$$

Where x and y indicate the distance from the center of one pixel to the center of an adjacent pixel in the X and Y axes respectively. It is determined by squared ratio of the CT image field of view to the image array size (512×512). The image parameters of the provided dataset; pixel spacing, thickness, and voxel size were ($0.703/0.703$), 2.5 and 1.235 respectively. Fig. 12, shows the centered pixels of lung's nodules were labeled with two colors: red and green that represented actual center that was recognized by radiologist and the determined center by the proposed system. The black and blue colors show the overlapped area between clusters in different slices, and the remaining pixels of the cluster areas respectively. Generally, the plotted volumetric lung's nodules by the Polt.ly application and 3D-DBSCAN methods proved the efficacy of the suggested system in this study. Where, all used methods described accurately the connected regions between linked nodules in CT lung scans.

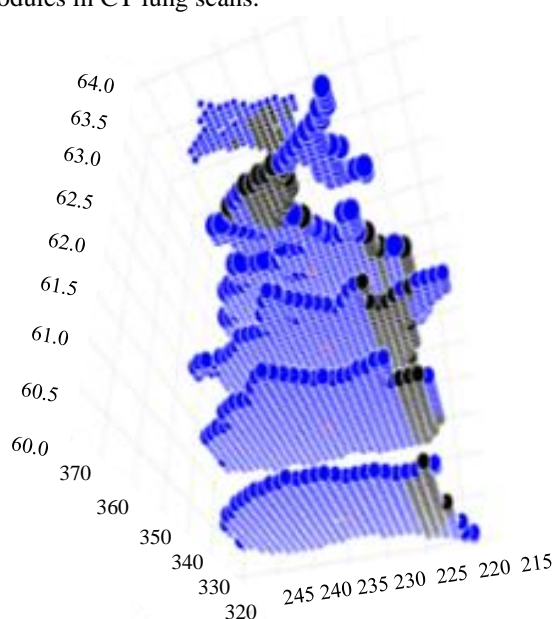


Fig. 10. Three-dimensional Plot of lung's Nodules was distributed on Different Levels from Slice 60 to 64

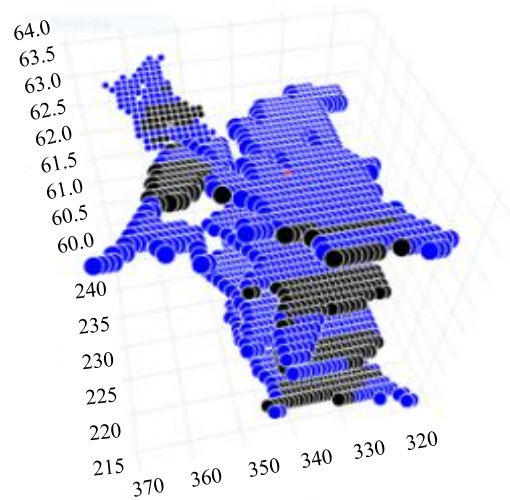


Fig. 11. Three-dimensional Plot of lung's nodule of the same case in Fig.10 but from different view, Black Bubbles Represent the Overlapping between Nodules to Show the Connected Regions

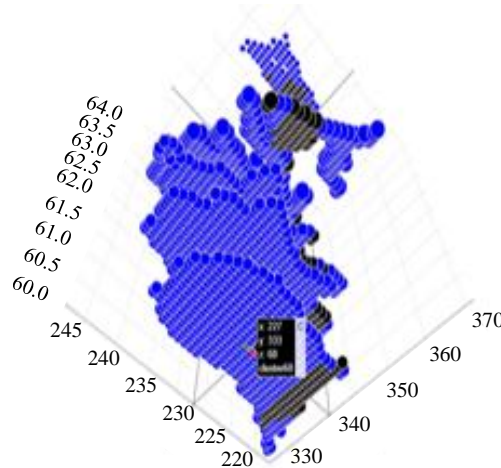


Fig. 12. The Overlapping between Centre Pixels of Clustered and Actual Nodule in the 60 Slice with Two Colors Red and Green Respectively

Discussion and Conclusions. The main objective of this paper was to build and implement a fully automated algorithm to describe the pulmonary nodules in CT lung images regarding shape and location matching the radiologist's report. The proposed method could cluster the nodules and showed their shape, location, type, and progress within the lung organ. The final algorithm outcomes and case study were evaluated by other 3D clustering methods emphasizing the accurate research results. This work is performed within several stages, with different methods are used for this purpose. Firstly, threshold and K-means clustering segment the nodules and vessels of CT lung images as objects with high intensity in 2D images. With 3D function, the 2D clustered images are stacked to display the nodule progress in 3D view. The algorithm results were validated by matching the center pixels of detected nodules by 3D Clustering and actual nodules reported by radiologists. In addition, the study identified a complicated case in the data, which is suspected the radiologists may miss because it was invisible. In this case, the algorithm proves and shows an attachment between two nodules making the nodules as one nodule against the radiologist's report. The evaluation stage has been done by applying the 3D-DBSCAN and 3D application methods, which confirm the proposed method results precision for this work. The Clustering of 3D-DBSCAN demonstrates the number and location of nodules and reflects the nodule shape as far as to describe the type of nodule. Also, determining this case confirms the work abilities in the early detection of nodules, which provides a chance for recovery patient. Our algorithm has a promising result on the standard data of CT scan images in detecting the number and location of nodules, which correspond to radiologist report, and automatically providing nodule shape and type.

References

1. Hasan AM, AL-Jawad MM, Jalab HA, et al. Classification of Covid-19 Coronavirus, Pneumonia and Healthy Lungs in CT Scans Using Q-Deformed Entropy and Deep Learning Features. *Entropy*. 2020;22:517.

2. Magdy E, Zayed N, Fakhr M. Automatic Classification of Normal and Cancer Lung CT Images Using Multiscale AM-FM Features. International Journal of Biomedical Imaging. 2015;2015. <http://dx.doi.org/10.1155/2015/230830>
3. Hasan AM, Meziane F, Jalab HA (eds). Performance of Grey Level Statistic Features versus Gabor Wavelet for Screening MRI Brain Tumors: A Comparative Study. International Conference on Information Communication and Management (ICICM); 2016; UK: IEEE.
4. El-Bana S, Al-Kabbany A, Sharkas M. A Two-Stage Framework for Automated Malignant Pulmonary Nodule Detection in CT Scans. Diagnostics. 2020;10:131. <http://dx.doi.org/10.3390/diagnostics10030131>
5. Valente IRS, Cortez PC, Neto EC, et al. Automatic 3D Pulmonary Nodule Detection in CT Images: A Survey. Computer Methods and Programs in Biomedicine. 2016;124:91–107. <https://doi.org/10.1016/j.cmpb.2015.10.006>
6. Lederlin M, Revel M-P, Khalil A, et al. Management Strategy of Pulmonary Nodule in 2013. Diagnostic and Interventional Imaging. 2013;94:1081–1094. <https://doi.org/10.1016/j.diii.2013.05.007>
7. Netto SMB, Silva AC, Nunes RA, et al. Automatic Segmentation of Lung Nodules with Growing Neural Gas and Support Vector Machine. Computers in Biology and Medicine. 2012;42:1110–1021. <https://doi.org/10.1016/j.combiomed.2012.09.003>
8. Ma Z, Tavares JMR, Jorge RN (eds). A Review on the Current Segmentation Algorithms for Medical Images. Proceedings of the 1st International Conference on Imaging Theory and Applications (IMAGAPP); 2009.
9. Javaid M, Javid M, Rehman MZU, et al. A Novel Approach to CAD System for the Detection of Lung Nodules in CT Images. Computer Methods and Programs in Biomedicine. 2016;135:125–139. <https://doi.org/10.1016/j.cmpb.2016.07.031>
10. Fetita CI, Preteux F, Beigelman-Aubry C, et al. (eds). 3D Automated Lung Nodule Segmentation in HRCT. International Conference on Medical Image Computing and Computer-Assisted Intervention; 2003: Springer.
11. Ozekes S, Osman O. Computerized Lung Nodule Detection Using 3D Feature Extraction and Learning Based Algorithms. Journal of Medical Systems. 2010;34:185–194. <https://doi.org/10.1007/s10916-008-9230-0>
12. El-Baz A, Elnakib A, El-Ghar A, et al. Automatic Detection of 2D and 3D Lung Nodules in Chest Spiral CT Scans. International Journal of Biomedical Imaging. 2013;2013:517632. <https://doi.org/10.1155/2013/517632>
13. Bloch BN, Jain A, Jaffe CC. Data From BREAST-DIAGNOSIS. In: Archive TCI, ed. <http://doi.org/10.7937/K9/TCIA.2015.SDNROXXR2015>
14. Hamid A, Jalab, Rabha W, Ibrahim, Ali M, Hasan, et al. Medical Image Enhancement Based on Statistical Distributions in Fractional Calculus. IEEE Computing Conference 18-20 July 2017. United Kingdom, London; 2017.
15. Peter VJ, Karnan M. Medical Image Analysis Using Unsupervised and Supervised Classification Techniques. International Journal of Innovative Technology and Exploring Engineering. 2013;3:40–45.
16. Rajaraman A, Ullman JD. Mining of Massive Datasets. Cambridge University Press; 2011.
17. Celebi ME, Kingravi HA, Vela PA. A Comparative Study of Efficient Initialization Methods for the K-Means Clustering Algorithm. Expert Systems with Applications. 2013;40:200–210. <https://doi.org/10.1016/j.eswa.2012.07.021>
18. Smith ST. MATLAB: Advanced GUI Development. Dog Ear Publishing; 2006.
19. Bankman I. Handbook of Medical Image Processing and Analysis. Elsevier; 2008.
20. Papademetris X, Joshi A. An Introduction to Programming for Medical Image Analysis with the Visualization Toolkit. Yale University. 2006;283.
21. Sander J, Ester M, Kriegel H-P, et al. Density-Based Clustering in Spatial Databases: The Algorithm GDBSCAN and Its Applications. Data Mining and Knowledge Discovery. 1998;2:169–194.
22. Kriegel HP, Kröger P, Sander J, et al. Density-Based Clustering. Wiley Interdisciplinary Reviews: Data Mining and Knowledge Discovery. 2011;1(3):231–240. <https://doi.org/10.1002/widm.1343>
23. Schubert E, Sander J, Ester M, et al. DBSCAN Revisited, Revisited: Why and How You Should (Still) Use DBSCAN. ACM Transactions on Database Systems (TODS). 2017;42(3):1–21. <https://doi.org/10.1145/3068335>

Received 08.08.2022

Revised 29.08.2022

Accepted 30.08.2022

About the Authors:

Al-Funjan, Amara, Lecturer in Mathematics Department, College of Pure Sciences, Babylon University (PO Box 4 Hilla City, Babylon, 51001, Iraq). Ph.D, [ResearcherID](#), [ORCID](#), amara.alfunjan@uobabylon.edu.iq

Meziane, Farid, College of Science and Engineering, School of Computing and Engineering, University of Derby (DE22 1GB, Derby, UK), Ph.D, [ScopusID](#), [ORCID](#), f.meziane@derby.ac.uk

Aspin, Rob, Deputy Head, Manchester Metropolitan University, (M15 6BH, Manchester, UK), Ph.D, [ScopusID](#), [ORCID](#), R.Aspin@mmu.ac.uk

Claimed contributorship:

A. Al-Funjan: conception, design and drafting the manuscript and acquisition of data and analysis. F. Meziane: interpretation, revision and proofreading. R. Aspin: formal analysis.

Conflict of interest statement

The authors do not have any conflict of interest.

All authors have read and approved the final manuscript.